Food Chemistry: X 16 (2022) 100477

Contents lists available at ScienceDirect

Food Chemistry: X

journal homepage: www.sciencedirect.com/journal/food-chemistry-x

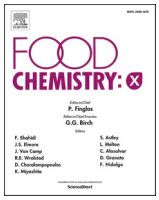

Fabrication, characterization of carboxymethyl konjac glucomannan/ovalbumin-naringin nanoparticles with improving *in vitro* bioaccessibility

Weimin Tang [a,b,1], Yanjun Wei [b,1], Wenjing Lu [b], Di Chen [b], Qin Ye [b], Cen Zhang [b], Yufeng Chen [a,c,*], Chaogeng Xiao [b,*]

[a] *National Engineering Research Center for Optical Instruments, College of Optical Science and Engineering, College of Biosystems Engineering and Food Science, Zhejiang University, Hangzhou, Zhejiang 310052, China*
[b] *State Key Laboratory for Managing Biotic and Chemical Threats to the Quality and Safety of Agro-products, Food Science Institute, Zhejiang Academy of Agricultural Sciences, Hangzhou, Zhejiang 310021, China*
[c] *College of Food Science and Technology, Zhejiang University of Technology, Hangzhou, Zhejiang 310014, China*

ARTICLE INFO

Keywords:
Flavanone
Bioavailability Enhancement
Nano-delivery system
Water Solubility
Fluorescence Intensity
Encapsulation efficiency (EE)

ABSTRACT

Naringin is potential functional and therapeutic ingredient, has low bioavailability because of poor aqueous solubility. In this study, an ovalbumin (OVA)-carboxymethyl konjac glucomannan (CKGM) nano-delivery system was developed to enhance the bioavailability of naringin. The effects of proportion (OVA: CKGM), pH and naringin concentration were studied on the formation, encapsulation efficiency (EE) and bioaccessibility of OVA/CKGM-Naringin nanoparticles (OVA/CKGM-Naringin NPs). Its morphology and size were viewed by Scanning Electron Microscope (SEM) and Transmission Electron Microscopy (TEM). The cross-linkage between OVA and CKGM was verified by Fourier Transform Infrared Spectroscopy (FTIR) and Fluorescence Intensity analysis. The size of OVA/CKGM-Naringin NPs were 463.83 ± 18.50 nm (Polydispersity Index-PDI, 0.42 ± 0.05). It indicated that 2:1 of OVA: CKGM, pH 3 and 7 mg/mL of naringin concentration were optimized processing parameters of OVA/CKGM-Naringin NPs with EE (97.90 ± 2.97 %) and remarkably improved bioaccessibility (85.01 ± 2.52 %). The OVA/CKGM-Naringin NPs was energy efficiently prepared and verified as an ideal carrier of naringin.

Introduction

As a member of flavanone family, naringin (Fig. 1a) is mainly extracted from the cirtus species with chemical name as 4′, 5, 7-trihydroxyflflavanone 7-rhamnoglucoside (Cavia-Saiz et al., 2010). It possesses a great many potential treatments, like the remission effect on LPS-induced myocardial dysfunction (Sun et al., 2019), promoting the peripheral nerve regeneration, which was verified in *In Vitro* and *In Vivo* modes (Ebrahimi et al., 2020) and the anti-inflammatory in various spices inducing mode (Pleguezuelos-Villa et al., 2018). An increasing number of researches are intended to reveal the great potential therapeutic effects of naringin as phytochemical (Gong et al., 2020; Salehi et al., 2019). Salman Ahmed et al. has reviewed the potential therapeutic effects of naringin on neurological disorders (Ahmed, Khan, Aschner, Hasan, & Hassan, 2019). However, the applications of naringin in food and biopharmaceutical fields are greatly restricted by its poor solubility in aqueous system and bitterness taste (Tang & Yan, 2016), which restricted its bioavailability and direct usage in beverage and milk products without any adjustment. So numerous bioactivities of naringin are achieved by high dose of naringin which further lead to a big waste of bioresource and threat to human health. And also, some indigestible flavonoids partly reach the colon and be mediated by localized microbiome (Cassidy & Minihane, 2017; Gong et al., 2018).

Nano-encapsulation is developing as a new way for protecting some functional compounds which are sensitive to pH and thermal (Chen et al., 2022). Polyphenols were encapsulated into chitosan-tripolyphosphate nanoparticles to improve its bioavailability of functional food ingredients (Di Santo, D Antoni, Domínguez Rubio, Alaimo, & Pérez, 2021; Milinčić et al., 2019). And also, the biopharma ingredients, such as prednisolone acetate (Hanafy et al., 2019) and

* Corresponding authors at: State Key Laboratory for Managing Biotic and Chemical Threats to the Quality and Safety of Agro-products, Food Science Institute, Zhejiang Academy of Agricultural Sciences, Hangzhou, Zhejiang 310021, China. National Engineering Research Center for Optical Instruments, College of Optical Science and Engineering; College of Biosystems Engineering and Food Science, Zhejiang University, Hangzhou, Zhejiang 310052, China.
E-mail addresses: swiven@163.com (W. Tang), wyj3893302@163.com (Y. Wei), wuyycyf@163.com (Y. Chen), xiaochaogeng@163.com (C. Xiao).
[1] Co-first author.

https://doi.org/10.1016/j.fochx.2022.100477
Received 31 May 2022; Received in revised form 20 September 2022; Accepted 12 October 2022
Available online 13 October 2022

albendazole (Kang et al., 2017).

Actually, nanotechnology has been used for encapsulating naringin (Feng et al., 2017) or together with other bioactive components (Ebrahimi et al., 2020) with good releasing efficiency but low encapsulation efficiency (<60 %). After being encapsulated into nanoparticles, the physiological activities of naringin could be achieved by relatively smaller amount, avoiding bioresource wasting and side effects induced by high dosage.

Protein and polysaccharides, as representative biodegradable biopolymers with native bioactivities for human health, had been proved as ideal encapsulation wall materials for food and pharmaceutical purposes (Chen et al., 2021). Ovalbumin, the major protein of egg white, can be used as nanoparticles wall materials through self-crosslinking by its positive NH^{3+} (Gou et al., 2018; Visentini, Perez, & Santiago, 2019) or mixed together with other materials, such as carboxymethylcellulose, cashew gum and κ-carrageenan (Gomez-Estaca, Comunian, Montero, Ferro-Furtado, & Favaro-Trindade, 2016; Xie et al., 2019; Xiong, Ren, Li, & Li, 2018). Polysaccharides are benefit in restraining OVA protein aggregation (Chen et al., 2021). For example, CKGM has showed good encapsulation ability with bovine serum albumin (Du et al., 2005). Because of rich $–COO^-$ in acid environment, CKGM could crosslink with positive ionic matrix by electronic interaction (Cao, Huang, Li, Guo, & Xiao, 2021).

OVA and CKGM were adopted to fabricate naringin nano-delivery system to enhance bioaccessibility of naringin by improving the encapsulation efficiency and crosslinking degree at room temperature. The pH, proportion of OVA: CKGM and naringin concentration were evaluated by comparing EE. As a result, the relative optimal parameters were screened out, including 2:1 (OVA: CKGM), pH 3 and 7 mg/mL of naringin concentration. The preparation of OVA/CKGM-Naringin NPs was conducted under room temperature which could be an energy conserved processing way in the background of global carbon emission reduction. Besides, mild processing temperature is benefit for embedding other heat sensitive natural products by OVA/CKGM nano-delivery system. High temperature (above 40 °C) generally promotes a serial reaction among chemical groups of CKGM and OVA, self-aggregation of OVA. The usage of high temperature treated materials were restricted due to their irreversible reactions.

In this study, the FTIR was used to analyze the chemical group interactions between different groups. The intrinsic fluorescence intensities were determined to assess the interaction between OVA and CKGM after being mixed in different portions. At the same time, the *In Vitro* mode was adopted to assess bioaccessibility of different groups, the selected combination was verified that it can be efficiently improve naringin bioaccessibility in simulated biofluids, including simulated gastric fluid (SGF) and simulated intestinal fluid (SIF). In present study, OVA/CKGM-Naringin NPs nano-delivery system was verified as efficient carrier of naringin which can also be used for other functional components encapsulation in food, cosmetic and pharmaceutical fields in the future.

Material and methods

Material and chemical reagents

Naringin (purity > 98 %) was bought from Sigma Aldrich. Carboxymethyl Modified Konjac Glucomannan (CKGM) was purchased from Shaanxi Sweden Biotechnology Co., ltd. Ovalbumin (OVA) was purchased from Sangon Biotech (Shanghai) Co., ltd. Pepsin (from porcine stomach mucose) and pancreatin (from porcine pancreas) were bought from Shanghai yuanye Bio-Technology Co., ltd. Hydrogen chloride (HCl) and sodium hydroxide (NaOH), and potassium hydroxide (KOH) were bought from Sinopharm Chemical Reagent Group Co. ltd. All other chemical used were of analytical reagent.

Preparation of OVA/CKGM-Naringin NPs

The OVA/CKGM-Naringin NPs were prepared as method in reference with minor modifications (Xie et al., 2019). Predetermined concentrations (w/v) of OVA and CKGM were individually dissolved with distilled water and then stored in 4 °C refrigerator for further use. Then naringin standard solutions in ethanol (5, 7 and 12 mg/mL, w/v) were prepared, 2 mL of which was pipetted and thoroughly mixed with OVA (30 mL) as prepared above and was further stirred for 20 min. The addition of ethanol (2 mL, 6.6 % v/v) to promote the dissolution of naringin in standard solution, however, the influence of residual ethanol on the

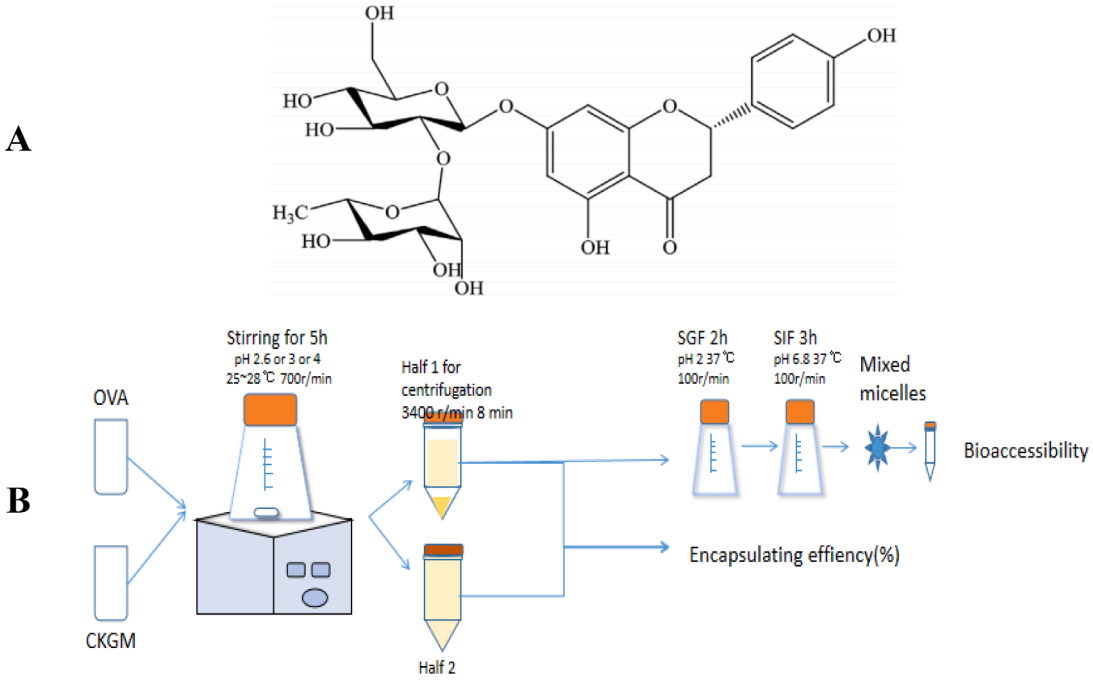

Fig. 1. Chemical structure of naringin (a) and flow chart of preparing process (b).

solubility of naringin in the system can be ignored because it is almost evaporated after being agitated for 5 h over 35 °C. After the addition of CKGM (30 mL) as prepared above, the pH of mixed solution was adjusted accordingly to 2.6, 3.0 and 4.0. After being magnetically stirred for 5 h at 700 rpm, the mixed solution was crosslinked in 4 °C refrigerator for at least 8 h. Finally, the solution was equally divided into two parts for calculating encapsulation efficiency (EE) and bioaccessibility of naringin. One part is for centrifugation (3400 rpm, 8 min) to remove non-encapsulated naringin, and the supernate was marked as N_L, concentration in this part refers to those encapsulated naringin, and the other part was marked as N_W as showed in Eq. (2).

Determination for naringin content

Naringin standard solutions (5 mg/mL, in methanol) were prepared with triplicates. Serial volumes (0.0, 0.4, 0.6, 0.8, 1.0 and 1.2 mL) of naringin standard solution (5 mg/mL) were pipetted respectively and each mixed with 0.5 mL 10 % aqueous KOH to obtain reaction solutions of different naringin concentrations. After color rendering for 5 min, each solution was isovolumetrically volumed to 10 mL with methanol. Then the absorbance of each solution was measured by UV spectrometer (Spectra Max 190, Molecular Devices, USA) at the wave length of 415 nm (λ). The regression equation (Eq. (1), $R^2 = 0.9964$) was obtained according to linear fitting between the absorbance and the concentration. The naringin content could be calculated according to Eq. (1), in which X, Y refers to the naringin concentration and UV absorbance respectively. The results of naringin content are benefit of further calculation of encapsulation efficiency and bioaccessibility.

$$Y = 0.0336X + 0.0133 \quad (R^2 = 0.9964) \tag{1}$$

Encapsulation efficiency (EE) analysis

As showed in processing flow chart, the same volume of solutions (half 1 and half 2 in Fig. 1b) was fetched from two parts and diluted with double volume of absolute ethanol. The solutions were vortexed for 2 min and centrifuged 3400 rpm for 8 min. The supernatant (1.0 mL) was fetched and blown to dry with nitrogen, and finally the residues with naringin were dissolved with 1.0 mL of methanol for absorbance determination by UV spectra at λ (415 nm) and the naringin content was calculated.

The encapsulation efficiency was calculated from the proportion of naringin in the supernate, marked N_L to the total naringin (without centrifugation), marked as N_W in the following equation (Eq. (2)):

$$EE(\%) = \frac{N_L}{N_W} \times 100\% \tag{2}$$

Bioaccessibility analysis

Two kinds of simulated digestion fluids including the simulated gastric fluid (SGF) and simulated intestinal fluid (SIF) were prepared according to the Chinese pharmacopoeia (2015 version). SGF was mainly composed of pepsin and HCl in the pH range of 1–2. Pepsin (10.000 g) was dissolved with 16.4 mL 16.4 mol/L hydrochloric acid and metered final volume to 1000 mL. SIF was composed of pancreatin in pH 6.8 condition. Monopotassium phosphate (6.800 g) were precisely weighted and dissolved in 500 mL distilled water. The pH of the solution was adjusted to 6.8 by adding 0.1 mol/L sodium hydroxide and metered final volume to 1000 mL. Sample liquid (3 mL) was mixed with 3 mL of SGF and 100 rpm shaked for 2 h. Then, the pH was adjusted to 6.8, then SIF (6.0 mL) was added into the mixture and shaked for another 3 h. The digested fluid (1.5 mL) was fetched and dissolved with ethanol. After being vortexed for 5 min, the mixed digested fluid was centrifuged at 3400 rpm for 8 min. Supernate (1.0 mL) was pipetted and combined with 4.5 mL methanol as reaction sample solution. The methanol only and naringin were used as blank, positive control respectively, the absorbance of which were obtained by the same procedure as in 2.3 Determination for naringin content.

Bioaccessibility of bioactive components referring to the part that is released from the matrix into the gastrointestinal tract while it is being digested, absorbed and transported to different parts of human body according to definition (Anal, Shrestha, & Sadiq, 2019). The bioaccessibility of naringin could be calculated according to the equation as mentioned in references (Chen et al., 2020; Schulz et al., 2017). This is a very important index to evaluate the bioavailability of the compound absorbed and used by human body (Kopec & Failla, 2018).

$$\text{Bioaccessibility}(\backslash\%)) = \frac{\text{Content of naringin released in the simulated digestion}}{\text{Content of naringin in the sample}} \times 100\% \tag{3}$$

Morphology analysis by SEM and TEM

The supernate of the centrifugated liquid was freeze dried for further morphology analysis by SEM and TEM. Before the observation for SEM, the freeze-dried sample was redissolved with distilled water, from which several samples were pipetted on the sample table and dried by infrared light, and then coated by an ion sputter (Q150T ES, Quorum, UK) with platinum under vacuum. The surface morphology of the nanoparticles was observed by using scanning electron microscopy (SU8010, Hitachi instruments, Tokyo, Japan) with voltage of 3 kV.

For TEM, the dried particles were redissolved with distilled water and then several droplets of sample were dropped onto copper grid. After being air dried for 3 ~ 5 min, the samples were observed by transmission electron microscope (H-7650, Hitachi Co., ltd, Japan).

Zeta potential, diameter and polydispersity index (PDI) analyses

The supernate of the centrifugated liquid was diluted with 8 times volumes of distilled water. The particle charge, particle size and PDI index of OVA/CKGM-Naringin NPs were determined by Nano-ZS 90 instrument (Malvern Instruments ltd, Worcestershire, UK) at room temperature.

Fluorescence intensity analysis

The intrinsic fluorescence intensity of different final concentrations of OVA (1 %, w/v) mixed with 0.1 %, 0.3 % and 0.5 % (w/v) of CKGM for 5 h at room temperature were obtained by F-2500 Fluorescence spectrum (Hitachi, Japan), the scanning spectrum ranges from 200 nm to 480 nm with the excitation wavelength of 280 nm and the same excitation and emission slit width (5 nm).

Fourier transform infrared (FTIR) analysis

The freeze-dried samples were analyzed with FTIR spectrometer (Vertex 70, Bruker Instrument Co., ltd, Germany). The FTIR spectra were obtain to investigate the interactions of chemical groups during the naringin encapsulation process. Freeze-dried samples were mixed with KBr and pressed into a thin plate for analyzation after the KBr background was surely removed.

Data analysis

All determinations were conducted in triplicate and the data were presented as the means ± standard deviations and analysis of variance was performed by using Origin2022b with multiple comparisons to verify the significant difference ($P < 0.05$,).

Results and discussion

Optimization of processing parameters by EE and bioaccessibility

OVA/CKGM-Naringin NPs were fabricated by the crosslinking of OVA and CKGM, two natural macromolecules. The preparation process needed 5 h to finish crosslinking between OVA and CKGM in room temperature. The prepared solutions were stored in refrigerator to enable them thoroughly swelled or crosslinked in 4 °C circumstances avoiding spoilage. In order to obtain optimal parameters of OVA/CKGM-Naringin NPs, processing parameters needed to be screened. Processing parameters including proportion of OVA: CKGM (5:1, 2:1 and 3:1), pH (2.6, 3.0 and 4.0) and naringin concentration (5, 7, 12 mg/mL, abbreviated as N5, N7 and N12) of OVA/CKGM-Naringin NPs preparation were optimized by comparing encapsulation efficiency (EE) and bioaccessibility among groups as shown in Fig. 2a-b. Bioaccessibility of OVA/CKGM-Naringin NPs prepared in different conditions and naringin as control is shown in Fig. 2b. Compared with the naked naringin powder (43.45 ± 1.88 %), the nano scale encapsulation method can enhance the bioaccessibility of naringin to approximately 85 %, which is similar with that of curcumin reported in reference (Jiang, Liao, & Charcosset, 2020).

As shown in Fig. 2a, it indicated that separately increased OVA amount of wall materials could not significantly enhance the EE of OVA/CKGM-Naringin NPs. Although 5: 1 pH 3 N5 (98.58 ± 1.26 %) showed the highest EE, there was no significant difference when compared with 3: 1 pH 3 N5 (94.47 ± 3.97 %) and 2:1 pH 3 N5 (88.75 ± 0.67 %). But too high proportion of OVA/CKGM significantly decreased bioaccessibility of naringin to 64.78 ± 4.69 % (5: 1 pH 3 N5). EE was enhanced by increasing OVA proportion is similar with the results of OVA/κ-carrageenan complex, in which OVA plays a vital role in the encapsulation process due to its good gelation ability and ideal physicochemical properties as wall materials (Xie et al., 2019), while high OVA lowered bioaccessibility. A relatively equivalent amounts (OVA: CKGM = 2:1) is recommended to maximally enable the crosslinking effect between OVA and CKGM. As mentioned in reference by Silva et al. (2019) that the wall material type, emulsifier and other factors may have impacts on the bioaccessibility. Also, the increasing wall materials increase EE (Feng et al., 2017).

It indicated from Fig. 2a that pH 2.6 (2:1 pH 2.6 N5) showed the lowest bioaccessibility of 69.48 ± 1.99 % when compared with 2:1 pH 3 N5 (80.80 ± 3.04 %) and 2:1 pH 4 N5 (84.53 ± 2.80 %). Obviously, increasing pH could promote bioaccessibility of fixed conditions (2:1 and N5), though showed no significant difference of EE among groups. The EE slightly increased from 86.68 ± 3.17 % (2:1 pH 2.6 N5) to 88.75 ± 0.67 % (2:1 pH 3 N5) when pH increased from 2.6 to 3.0, and further remarkably advanced to 94.40 ± 6.23 % (2:1 pH 4 N5) when pH was 4. CKGM possesses good cross-linking ability with chitosan for nano-encapsulation when pH approaching to 3.6, by which –COO^- groups will expose more outside (Du et al., 2005). This may be the reason of that 2:1 pH 4 N5 (94.39 ± 6.23 %) showed higher EE than 2:1 pH 2.6 N5 (86.68 ± 3.17 %) and 2:1 pH 3 N5 (88.75 ± 0.67 %). In order to avoid naringin degradation in high pH circumstance, pH 3.0 was chosen as proper factor.

Increasing loaded naringin to some extent could improve EE by fixing the proportion (2:1) and pH (3.0). The loaded naringin concentration of 7 mg/mL could greatly enhance the corresponding EE to 97.90 ± 2.97 % (2:1 pH 3 N7) compared with 5 mg/mL naringin concentration (2:1 pH 3 N5, 88.75 ± 0.68 %). However, EE decreased to 87.17 ± 0.62 % when naringin concentration was further increased to 12 mg/mL, which meant that the wall materials of OVA/CKGM were of overloaded status. The bioaccessibility of 2:1 pH 3 N12 (100 %) indicated that too much residual naringin existing outside of OVA and CKGM macromolecules. And some precipitations of naringin can be seen after being cooled overnight, which means that too high naringin concentration will decrease EE. Thus, 7 mg/mL was chosen as rational naringin concentration for preparing OVA/CKGM-Naringin NPs.

All above results indicated that the proportion of OVA: CKGM (2:1), pH 3.0 and naringin concentration (7 mg/mL) were recommended parameters for the fabrication of this nano-delivery system. Generally, in consideration of both EE (97.90 ± 2.97 %) and bioaccessibility (85.01 ± 2.52 %), 2:1, pH 3 and 7 mg/mL naringin will be the determined parameters in the OVA/CKGM-Naringin NPs manufacturing. The proportion of OVA: CKGM (2:1), pH 3.0 and naringin concentration of 7 mg/mL were optimized parameters for the fabrication of OVA/CKGM-Naringin NPs.

Zeta potential, diameter and polydispersity index (PDI) analysis

To make sure that the prepared nanoparticles could be greatly applied in food and biopharmaceutical industries, the liquid stability and drug releasing behavior are very important indexes to be assessed. Therefore, particle size and distribution, surface charge are key indicators for evaluating these characteristics (Hu et al., 2016). For particles distribution uniformity, PDI is a very important parameter to be evaluated (Nallamuthu, Ponnusamy, Smruthi, & Khanum, 2021).

As we know, the isoelectric point of OVA falls in the range of 4.59–4.71, around which OVA could easily form particle by protein aggregation. In pH 3 condition, OVA play a great role in self-aggregation showing positive charge and have electrostatic interaction with negative

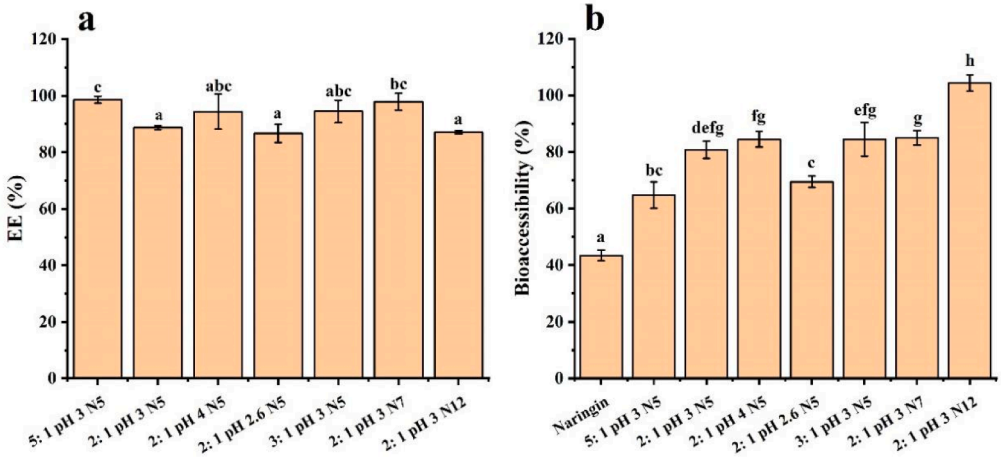

Fig. 2. EE (a) and bioaccessibility (b) of OVA/CKGM-Naringin NPs. ※: Different lowercase alphabet in figures representing significant difference ($P < 0.05$) between groups, one same lowercase alphabet means no significant difference ($P > 0.05$).

CKGM (Nallamuthu et al., 2021). We also found that the addition of naringin (5, 7, 12 mg/mL) hardly showed impact on the diameter and PDI of OVA/CKGM NPs, therefore naringin concentration was not taken into account in this assay. From Table 1, we can conclude that the diameters of OVA/CKGM NPs decreased with increasing proportion of OVA: CKGM from 2:1 to 3:1, 5:1 under the same pH condition. That is to say, increased OVA amount could effectively promote the formation of smaller OVA/CKGM NPs with good PDI value (0.36 ± 0.05) which is similar with reports by Gou et al. (2018). Actually, the EE is not only related to OVA mass percentage and particle size, but also with pH, it can be informed that there is a strong relationship between particle size and pH. OVA and CKGM can well cross-linked with each other at pH 3.0 with intermediate particle size compared with pH 2.6 and 4.0. There exists a positive relationship between EE and pH, which may due to the naringin dissolved more in alkaline solution, thus accordingly more naringin will be encapsulated into the particles. The 2:1 pH 3.0 has eligible PDI value (0.42 ± 0.01) which suggest narrow size distribution and homogeneous colloids by reference (Nallamuthu et al., 2021; Yuan et al., 2019). The value of all the liquid in this study are positive and similar to another reported CKGM-CS NPs (Du et al., 2005). CKGM could greatly inhibit self-aggregation of OVA contributing to good stability of nano-emulsion system.

SEM and TEM

Lyophilization is commonly used for desiccation of food processing materials and pharmaceutic preparation, which is a physical procedure triggered by the removal of water from solute. From the images of the SEM and TEM as shown in Fig. 3a and Fig. 3b, it can be seen that the outer formation is almost the same in different conditions. This finding indicates that the proportion of OVA: CKGM, pH and naringin concentration may have the similar morphological features. Both the SEM and TEM shows the round shape of the particles. And from the TEM, for the color and morphology, it's similar to the TEM images of other OVA related nanoparticles (Kim et al., 2016) and polysaccharides-protein nanoparticles (CS-OVA) (Zhang, Jiang, Huang, Li, & Wang, 2019). The nanoparticles diameters are approximately in the range of 200 ~ 300 nm, however, their diameters of TEM are relatively larger due to high moisture of samples. The diameters of particles in the liquid (380 ~ 600 nm, in Table 1) which are totally dissolved in water with hydraulic radius, while samples for TEM and SEM observations are freezing dried powders and redissolved in water in a few minutes to form smaller particle size.

Fluorescence intensity analysis

OVA is a single chain macromolecular protein (44.5 kDa) comprised of tyrosine and tryptophan with intrinsic fluorescence excited by 280 nm (Cheng et al., 2021). The finding of increased fluorescence intensity of OVA accompanied by declined concentration from 5 % to 1 % in Fig. 4a indicated that the OVA had self-quenching effect on the fluorescence intensity due to narrow molecular distance. CKGM, as another native macromolecule, show native fluorescence intensity at 384 nm due to its functional groups (C—O—C, —OH, C═O of the aldehyde group —CHO) (Xu, Li, He, Liao, & Chen, 2008), which can also be seen in other polysaccharide which is rich in oxygen unbonded electron generation of the other bond C—O—C has the emission (Dou, Chen, & Fu, 2019; He, Yu, Zhu, Gu, & Xu, 2006). After being blended with the CKGM, fluorescence intensity of OVA was increased by increasing CKGM concentration from 0.1 % to 0.5 %. This result is quite different from those of other scientists who consider maillard reaction between OVA of low concentration and sugars as the major reason. However, in present study, mild reaction temperature (RT) and big molecular weight of CKGM made it less possibility to finish maillard reaction in great extent. It was supposed that there existed electrostatic interaction in pH 3.0 between CKGM and OVA working as negative and positive respectively which contributed to structural changes of OVA and exposure of tyrosine showing strong fluorescence signals with wavelength shift<5 nm. Even though quenching condition can be seen in carboxymethyl cellulose-OVA, its relative high reaction temperature (60 °C) and low concentration of OVA were used in preparing process (Li et al., 2020). The combination of high concentration of 1 % OVA and 0.5 % CKGM show the strongest fluorescence intensity which mean there exist interaction between macromolecules to enhance the fluorescence intensity (Fig. 4b). That is to say, low and high concentration of OVA show inverse fluorescence behaviors. It could be more meaningful to investigate the crosslinking behavior of high OVA concentration system which is commonly used in beverage, milk, and other functional foods. Low processing temperature of OVA/CKGM-Naringin NPs is a promising energy conserved method that is used in treatment of high concentration matrix of OVA/CKGM.

Table 1
Diameter and PDI of OVA/CKGM NPs.

Groups	Z-average (nm)	Peak (nm)	Intensity	PDI
2:1 pH 2.6	409.20 ± 15.41^{b}	520.93 ± 36.59	96.13 ± 1.30	0.52 ± 0.08^{bcd}
2:1 pH 3.0	463.83 ± 18.50^{c}	533.20 ± 25.63	92.96 ± 2.62	0.42 ± 0.01^{ab}
2:1 pH 4.0	645.93 ± 11.73^{d}	637.83 ± 31.96	97.30 ± 1.26	0.56 ± 0.01 ^{cd}
3:1 pH 3.0	387.70 ± 9.13^{ab}	477.47 ± 5.60	96.87 ± 1.11	0.36 ± 0.05^{a}
5:1 pH 3.0	365.10 ± 11.23^{a}	417.40 ± 22.48	96.73 ± 1.58	0.60 ± 0.06^{d}

※: Different lowercase alphabet superscripted in table representing significant difference ($P < 0.05$) between groups, one same lowercase alphabet means no significant difference ($P > 0.05$).

FTIR analysis

The FTIR spectra can be seen from Fig. 5 that OVA/CKGM NPs and OVA/CKGM-Naringin NPs both have absorption peaks around 1650 cm^{-1}, indicating the interaction between the COO^{-} and the NH^{4+}, resulting in the formation of the amide bond, in the same range with those mentioned by Jian Du et al (Du et al., 2005). OVA/CKGM-Naringin NPs have relative sharp peak at 1656 cm^{-1}, but for the physical powder, there is no peak but at the 1637 cm^{-1} and the peak width is larger than that of the NPs. The COO^{-} and NH^{4+} have absorption in the range of 1475 ~ 1394 cm^{-1}, where OVA/CKGM-Naringin NPs and OVA/CKGM-Naringin NPs have relative flatter spectrum while OVA/CKGM physical mixture and OVA/CKGM-Naringin physical mixture have peaks. The absorption peaks at 1395 cm^{-1} and 1530 cm^{-1} were due to symmetric and asymmetric stretching vibration of COO^{-}, OVA/CKGM and OVA/CKGM-Naringin physically mixed samples have more sharp peaks in the range of 1396 ~ 1245 cm^{-1}, as many bonds are in free state in the physical powders, but OVA/CKGM NPs and OVA/CKGM-Naringin NPs have more flat peaks in this range, corresponding to the hydrophobic bonds or other linkages between the polymers, some bonds did not have absorption here. OVA/CKGM NPs and OVA/CKGM-Naringin NPs have relatively narrow absorbance compared with that of the physically mixed powder, the range (1396 ~ 1245 cm^{-1}) of which usually refer to the C—O stretching. It can be found that the interaction is more complex in the NPs. Naringin powder has sharp absorption peak at 887 and 819 cm^{-1}, the physically mixed powder without naringin do not has this absorbance but the physical powder with naringin has this sharp absorption at 887 and 819 cm^{-1}. There is no signal for OVA/CKGM-Naringin NPs which means that the naringin is encapsulated and cannot be clearly shown, which is in accordance with the previous report (Feng et al., 2017).

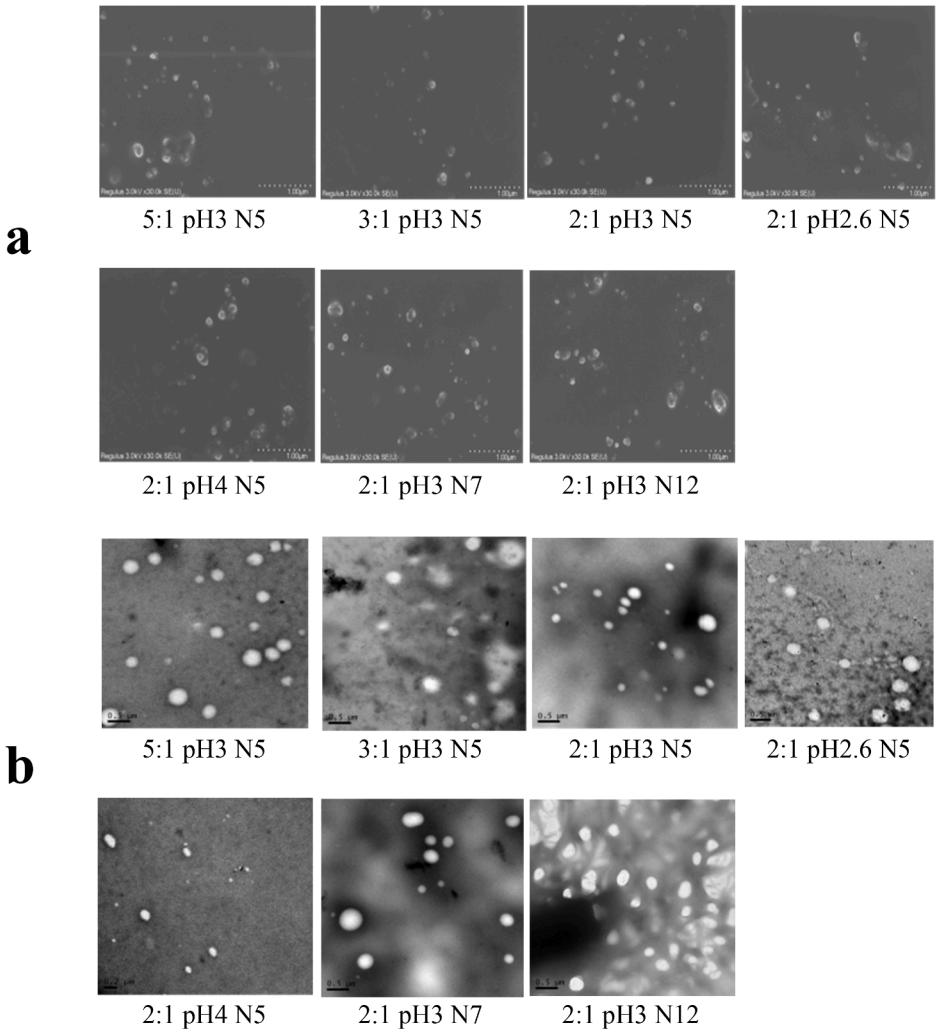

Fig. 3. SEM (a) and TEM (b) images of OVA/CKGM-Naringin NPs in different conditions.

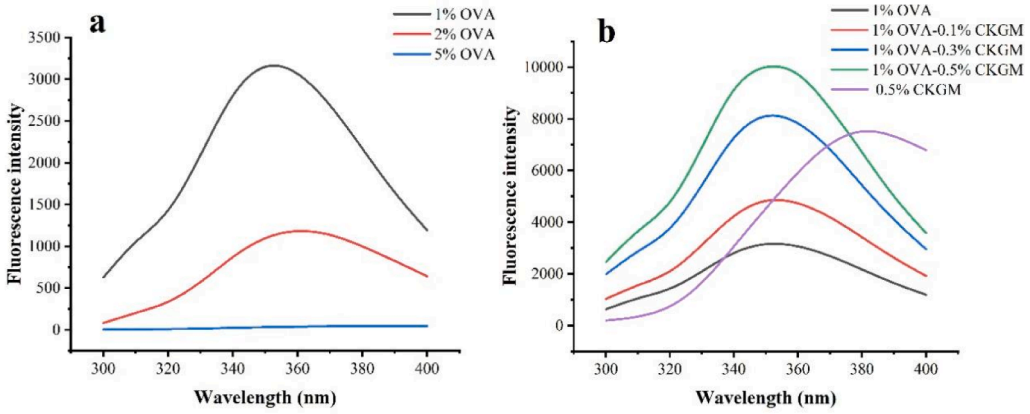

Fig. 4. Fluorescence intensity variation of 1 %, 2 % and 5 % OVA concentration (a) and 1 % OVA crosslinked with 0.1 %, 0.3 %, 0.5 % of CKGM (b).

Conclusion

In this study, the OVA/CKGM-Naringin NPs can be successfully prepared with encapsulation efficiency lager than 90 % with the diameter size around 200 ~ 600 nm. Considering of high EE and good bioaccessibility, the OVA: CKGM of 2:1, pH 3 and 7 mg/mL are optimized parameters. Fluorescence and FTIR could well indicate that the interaction between OVA and CKGM, which are potential wall materials for improving bioaccessibility of naringin to 85.01 ± 2.52 %. The high concentration OVA and CKGM matrixes of OVA/CKGM-Naringin NPs meet the requirements of nutrition feeding and fruit juice by working as nano-carrier to enhance the function of low water-soluble bioactive compounds. This is a promising nano-delivery system and green method for improving naringin absorption in digest tract enhancing the

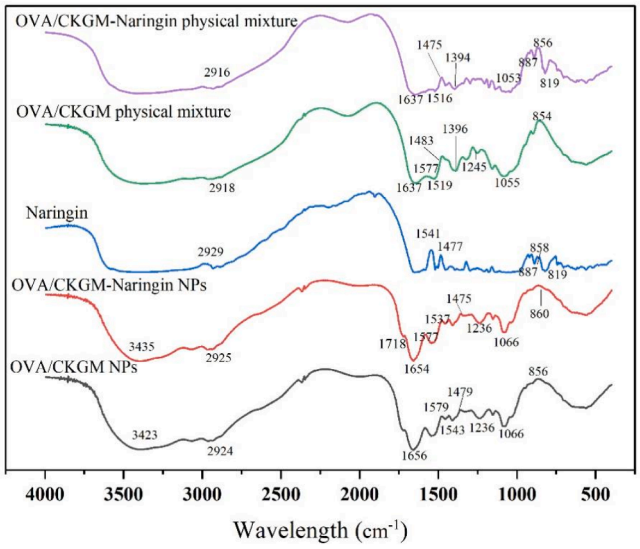

Fig. 5. FTIR spectra of different samples.

potential bio-utilization of naringin in food, biopharmaceutical industry in the future.

CRediT authorship contribution statement

Weimin Tang: Writing – original draft, Writing – review & editing. **Yanjun Wei:** Methodology, Writing – original draft, Writing – review & editing. **Wenjing Lu:** Methodology. **Di Chen:** Data curation. **Qin Ye:** Data curation. **Cen Zhang:** Writing – review & editing. **Yufeng Chen:** Conceptualization, Methodology, Writing – review & editing. **Chaogeng Xiao:** Writing – review & editing, Supervision, Project administration, Funding acquisition.

Declaration of Competing Interest

The authors declare that they have no known competing financial interests or personal relationships that could have appeared to influence the work reported in this paper.

Acknowledgments

This work was financially supported by Zhejiang Province Public Welfare Technology Application Research Project (Grant No: LGJ21C20001), the Zhejiang Provincial Key Research and Development Program (Grant No: 2022C02064) and Key Laboratory of Marine Fishery Resources Exploitment & Utilization of Zhejiang Province (Grant No: SL2022004). We are also grateful to internal funding of Zhejiang Academy of Agricultural Sciences for youth scholars directed by Weimin Tang.

References

Ahmed, S., Khan, H., Aschner, M., Hasan, M. M., & Hassan, S. T. S. (2019). Therapeutic potential of naringin in neurological disorders. *Food and Chemical Toxicology, 132*, Article 110646.

Anal, A. K., Shrestha, S., & Sadiq, M. B. (2019). Biopolymeric-based emulsions and their effects during processing, digestibility and bioaccessibility of bioactive compounds in food systems. *Food Hydrocolloids, 87*, 691–702.

Cao, Y., Huang, G., Li, X., Guo, L., & Xiao, J. (2021). Complex coacervation of carboxymethyl konjac glucomannan and ovalbumin and coacervate characterization. *Journal of Dispersion Science and Technology*, 1–11.

Cassidy, A., & Minihane, A. (2017). The role of metabolism (and the microbiome) in defining the clinical efficacy of dietary flavonoids. *The American Journal of Clinical Nutrition, 105*(1), 10–22.

Cavia-Saiz, M., Busto, M. D., Pilar-Izquierdo, M. C., Ortega, N., Perez-Mateos, M., & Muñiz, P. (2010). Antioxidant properties, radical scavenging activity and biomolecule protection capacity of flavonoid naringenin and its glycoside naringin: A comparative study. *Journal of The Science of Food and Agriculture, 90*(7), 1238–1244.

Chen, Y., Peng, J., Wang, Y., Wadhawan, D., Wu, L., Gao, X., … Xia, G. (2021). Development, Characterization, Stability and Bioaccessibility Improvement of 7,8-Dihydroxyflavone Loaded Zein/Sophorolipid/Polysaccharide Ternary Nanoparticles: Comparison of Sodium Alginate and Sodium Carboxymethyl Cellulose. *Foods, 10*(11), 2629.

Chen, Y., Sun, Y., Ding, Y., Ding, Y., Liu, S., Zhou, X., … Lu, B. (2022). Recent progress in fish oil-based emulsions by various food-grade stabilizers: Fabrication strategy, interfacial stability mechanism and potential application. *Critical Reviews in Food Science and Nutrition*, 1–24.

Chen, Y., Xia, G., Zhao, Z., Xue, F., Chen, C., & Zhang, Y. (2020). Formation, structural characterization, stability and in vitro bioaccessibility of 7,8-dihydroxyflavone loaded zein-/sophorolipid composite nanoparticles: Effect of sophorolipid under two blending sequences. *Food & Function, 11*(2), 1810–1825.

Cheng, W., Ma, J., Wang, S., Lou, R., Wu, S., He, J., … Xiao, F. (2021). Interaction mechanism between resveratrol and ovalbumin based on fluorescence spectroscopy and molecular dynamic simulation. *LWT- Food Science and Technology, 146*(2021), Article 111455.

Di Santo, M. C., D Antoni, C. L., Domínguez Rubio, A. P., Alaimo, A., & Pérez, O. E. (2021). Chitosan-tripolyphosphate nanoparticles designed to encapsulate polyphenolic compounds for biomedical and pharmaceutical applications – A review. *Biomedicine & Pharmacotherapy, 142*, Article 111970.

Dou, Z., Chen, C., & Fu, X. (2019). The effect of ultrasound irradiation on the physicochemical properties and α-glucosidase inhibitory effect of blackberry fruit polysaccharide. *Food Hydrocolloids, 96*, 568–576.

Du, J., Sun, R., Zhang, S., Zhang, L., Xiong, C., & Peng, Y. (2005). Novel polyelectrolyte carboxymethyl konjac glucomannan-chitosan nanoparticles for drug delivery. I. Physicochemical characterization of the carboxymethyl konjac glucomannan-chitosan nanoparticles. *Biopolymers, 78*(1), 1–8.

Ebrahimi, M. H., Samadian, H., Davani, S. T., Kolarijani, N. R., Mogharabian, N., Salami, M. S., & Salehi, M. (2020). Peripheral nerve regeneration in rats by chitosan/alginate hydrogel composited with Berberine and Naringin nanoparticles: In vitro and in vivo study. *Journal of Molecular Liquids, 318*, Article 114226.

Feng, T., Wang, K., Liu, F., Ye, R., Zhu, X., Zhuang, H., & Xu, Z. (2017). Structural characterization and bioavailability of ternary nanoparticles consisting of amylose, α-linoleic acid and β-lactoglobulin complexed with naringin. *International Journal of Biological Macromolecules, 99*, 365–374.

Gomez-Estaca, J., Comunian, T. A., Montero, P., Ferro-Furtado, R., & Favaro-Trindade, C. S. (2016). Encapsulation of an astaxanthin-containing lipid extract from shrimp waste by complex coacervation using a novel gelatin–cashew gum complex. *Food Hydrocolloids, 61*, 155–162.

Gong, L., Cao, W., Chi, H., Wang, J., Zhang, H., Liu, J., & Sun, B. (2018). Whole cereal grains and potential health effects: Involvement of the gut microbiota. *Food Research International, 103*, 84–102.

Gong, L., Feng, D., Wang, T., Ren, Y., Liu, Y., & Wang, J. (2020). Inhibitors of α-amylase and α-glucosidase: Potential linkage for whole cereal foods on prevention of hyperglycemia. *Food Science & Nutrition, 8*(12), 6320–6337.

Gou, S., Chen, Q., Liu, Y., Zeng, L., Song, H., Xu, Z., … Xiao, B. (2018). Green Fabrication of Ovalbumin Nanoparticles as Natural Polyphenol Carriers for Ulcerative Colitis Therapy. *ACS Sustainable Chemistry & Engineering, 6*(10), 12658–12667.

Hanafy, A. F., Abdalla, A. M., Guda, T. K., Gabr, K. E., Royall, P. G., & Alqurshi, A. (2019). Ocular anti-inflammatory activity of prednisolone acetate loaded chitosan-deoxycholate self-assembled nanoparticles. *International Journal of Nanomedicine, 14*, 3679–3689.

He, H., Yu, R., Zhu, T., Gu, Z., & Xu, H. (2006). Study of Fluorescence Spectra of Starch Suspension. *Spectroscopy and Spectral Analysis, 26*(9), 1636–1639.

Hu, D., Xu, Z., Hu, Z., Hu, B., Yang, M., & Zhu, L. (2016). pH-Triggered Charge-Reversal Silk Sericin-Based Nanoparticles for Enhanced Cellular Uptake and Doxorubicin Delivery. *ACS Sustainable Chemistry & Engineering, 5*(2), 1638–1647.

Jiang, T., Liao, W., & Charcosset, C. (2020). Recent advances in encapsulation of curcumin in nanoemulsions: A review of encapsulation technologies, bioaccessibility and applications. *Food Research International, 132*, Article 109035.

Kang, B., Choi, J., Lee, S., Lee, J., Kim, T., Jang, W. S., … Park, J. (2017). Enhancing the in vitro anticancer activity of albendazole incorporated into chitosan-coated PLGA nanoparticles. *Carbohydrate Polymers, 159*, 39–47.

Kim, S., Phuengkham, H., Noh, Y., Lee, H., Um, S. H., & Lim, Y. T. (2016). Immune Complexes Mimicking Synthetic Vaccine Nanoparticles for Enhanced Migration and Cross-Presentation of Dendritic Cells. *Advanced Functional Materials, 26*(44), 8072–8082.

Kopec, R. E., & Failla, M. L. (2018). Recent advances in the bioaccessibility and bioavailability of carotenoids and effects of other dietary lipophiles. *Journal of Food Composition and Analysis, 68*, 16–30.

Li, Z., Kuang, H., Yang, J., Hu, J., Ding, B., Sun, W., & Luo, Y. (2020). Improving emulsion stability based on ovalbumin-carboxymethyl cellulose complexes with thermal treatment near ovalbumin isoelectric point. *Scientific Reports, 10*(1).

Milinčić, D. D., Popović, D. A., Lević, S. M., Kostić, A. Z., Tešić, Z. L., Nedović, V. A., & Pešić, M. B. (2019). Application of polyphenol-loaded nanoparticles in food industry. *Nanomaterials, 9*(11), 1629.

Nallamuthu, I., Ponnusamy, V., Smruthi, M. R., & Khanum, F. (2021). Formulation of naringin encapsulation in zein/caseinate biopolymers and its anti-adipogenic activity in 3T3-L1 pre-adipocytes. *Journal of Cluster Science, 32*(6), 1649–1662.

Pleguezuelos-Villa, M., Mir-Palomo, S., Díez-Sales, O., Buso, M. A. O. V., Sauri, A. R., & Nácher, A. (2018). A novel ultradeformable liposomes of Naringin for anti-inflammatory therapy. *Colloids and Surfaces B: Biointerfaces, 162*, 265–270.

Salehi, B., Fokou, P., Sharifi-Rad, M., Zucca, P., Pezzani, R., Martins, N., & Sharifi-Rad, J. (2019). The therapeutic potential of naringenin: A review of clinical trials. *Pharmaceuticals, 12*(1), 11.

Schulz, M., Biluca, F. C., Gonzaga, L. V., Borges, G. D. S. C., Vitali, L., Micke, G. A., … Fett, R. (2017). Bioaccessibility of bioactive compounds and antioxidant potential of juçara fruits (Euterpe edulis Martius) subjected to in vitro gastrointestinal digestion. *Food Chemistry, 228*, 447–454.

Silva, H. D., Beldíková, E., Poejo, J., Abrunhosa, L., Serra, A. T., Duarte, C. M. M., … Vicente, A. A. (2019). Evaluating the effect of chitosan layer on bioaccessibility and cellular uptake of curcumin nanoemulsions. *Journal of Food Engineering, 243*, 89–100.

Sun, L., Qiao, W., Xiao, Y., Cui, L., Wang, X., & Ren, W. (2019). Naringin mitigates myocardial strain and the inflammatory response in sepsis-induced myocardial dysfunction through regulation of PI3K/AKT/NF-κB pathway. *International Immunopharmacology, 75*, Article 105782.

Tang, N., & Yan, W. (2016). Solubilities of naringin dihydrochalcone in pure solvents and mixed solvents at different temperatures. *Journal of Chemical & Engineering Data, 61*(12), 4085–4089.

Visentini, F. F., Perez, A. A., & Santiago, L. G. (2019). Self-assembled nanoparticles from heat treated ovalbumin as nanocarriers for polyunsaturated fatty acids. *Food Hydrocolloids, 93*, 242–252.

Xie, H., Xiang, C., Li, Y., Wang, L., Zhang, Y., Song, Z., … Fang, W. (2019). Fabrication of ovalbumin/κ-carrageenan complex nanoparticles as a novel carrier for curcumin delivery. *Food Hydrocolloids, 89*, 111–121.

Xiong, W., Ren, C., Li, J., & Li, B. (2018). Characterization and interfacial rheological properties of nanoparticles prepared by heat treatment of ovalbumin-carboxymethylcellulose complexes. *Food Hydrocolloids, 82*, 355–362.

Xu, D., Li, G., He, X., Liao, Z., & Chen, X. (2008). Study on fluorescence spectral characteristics of dialdehyde konjac glucomannan solution. *Journal of Instrumental Analysis, 27*(12), 1273–1277.

Yuan, Y., Li, H., Liu, C., Zhang, S., Xu, Y., & Wang, D. (2019). Fabrication and characterization of lutein-loaded nanoparticles based on zein and sophorolipid: enhancement of water solubility, stability, and bioaccessibility. *Journal of Agriculture and Food Chemistry, 67*(43), 11977–11985.

Zhang, S., Jiang, H., Huang, S., Li, P., & Wang, F. (2019). Curdlan sulfate/O-linked quaternized chitosan nanoparticles acting as potential adjuvants promote multiple arms of immune responses. *Carbohydrate Polymers, 213*, 100–111.